AGU PUBLICATIONS

Geophysical Research Letters

RESEARCH LETTER
10.1002/2015GL064939

Key Points:
- OH rate coefficient measurements over the range 233 to 379 K
- UV spectrum measurements resolve existing discrepancies
- Experimental data and model calculations enable improved ODP and global warming potential estimates

Supporting Information:
- Figure S1, Tables S1–S5, and Caption for Data Set S1
- Data Set S1

Correspondence to:
J. B. Burkholder,
James.B.Burkholder@noaa.gov

Citation:
McGillen, M. R., F. Bernard, E. L. Fleming, and J. B. Burkholder (2015), HCFC-133a (CF_3CH_2Cl): OH rate coefficient, UV and infrared absorption spectra, and atmospheric implications, *Geophys. Res. Lett.*, *42*, 6098–6105, doi:10.1002/2015GL064939.

Received 12 JUN 2015
Accepted 2 JUL 2015
Accepted article online 3 JUL 2015
Published online 23 JUL 2015

HCFC-133a (CF_3CH_2Cl): OH rate coefficient, UV and infrared absorption spectra, and atmospheric implications

Max R. McGillen[1,2], François Bernard[1,2], Eric L. Fleming[3,4], and James B. Burkholder[1]

[1]Earth System Research Laboratory, Chemical Sciences Division, National Oceanic and Atmospheric Administration, Boulder, Colorado, USA, [2]Cooperative Institute for Research in Environmental Sciences, University of Colorado Boulder, Boulder, Colorado, USA, [3]NASA Goddard Space Flight Center, Greenbelt, Maryland, USA, [4]Science Systems and Applications, Inc., Lanham, Maryland, USA

Abstract HCFC-133a (CF_3CH_2Cl), an ozone-depleting substance, is primarily removed from the atmosphere by gas-phase reaction with OH radicals and by UV photolysis. The rate coefficient, k, for the OH + HCFC-133a reaction was measured between 233 and 379 K and is given by $k(T) = (9.32 \pm 0.8) \times 10^{-13} \exp(-(1296 \pm 28)/T)$, where k(296 K) was measured to be $(1.10 \pm 0.02) \times 10^{-14}$ (cm^3 $molecule^{-1}$ s^{-1}) (2σ precision uncertainty). The HCFC-133a UV absorption spectrum was measured between 184.95 and 240 nm at 213–323 K, and a spectrum parameterization is presented. The HCFC-133a atmospheric loss processes, lifetime, ozone depletion potential, and uncertainties were evaluated using a 2-D atmospheric model. The global annually averaged steady state lifetime and ozone depletion potential (ODP) were determined to be 4.45 (4.04–4.90) years and 0.017 (±0.001), respectively, where the ranges are based solely on the 2σ uncertainty in the kinetic and photochemical parameters. The infrared absorption spectrum of HCFC-133a was measured, and its global warming potential was determined to be 380 on the 100 year time horizon.

1. Introduction

The hydrochlorofluorocarbon CF_3CH_2Cl (HCFC-133a), a long-lived ozone-depleting substance (ODS) and potent greenhouse gas of anthropogenic origin, was recently detected in the atmosphere for the first time by *Laube et al.* [2014]. The atmospheric abundance of HCFC-133a was determined to be insignificant before the 1960s while increasing over the past 20 years to 0.37 parts per trillion (ppt) in 2012. HCFC-133a is used in the production of pharmaceuticals and is an intermediate in the production of hydrofluorocarbon HFC-134a (CF_3CH_2F) [*Manzer,* 1990*; Miller and Batchelor,* 2012*; United Nations Environment Programme,* 2012], although its emission into the atmosphere is not well known.

HCFC-133a has an estimated global atmospheric lifetime of 4.0 years [*World Meteorological Organization (WMO),* 2014] and is primarily removed from the atmosphere by gas-phase reaction with the OH radical in the troposphere. In the stratosphere, short-wavelength UV photolysis and to a lesser extent reaction with $O(^1D)$ are expected to contribute to its overall atmospheric removal. The current level of uncertainty in the OH + HCFC-133a reaction rate coefficient, k, which is estimated to be 30% (1σ) at 298 K by *Sander et al.* [2011], and the lack of kinetic data at temperatures <263 K limits the accuracy of atmospheric model estimates of the HCFC-133a atmospheric lifetime, ozone depletion potential (ODP), and global warming potential (GWP). Uncertainties in the UV absorption spectrum of HCFC-133a also contribute to this uncertainty but to a much lesser extent.

The rate coefficient for the OH + HCFC-133a reaction has been the subject of experimental investigations by *Howard and Evenson* [1976] (296 K), *Handwerk and Zellner* [1978] (263–373 K), *Clyne and Holt* [1979] (294–427 K), *Fang et al.* [1999] (295–866 K), and *DeMore* [2005] (298–360 K). Although the reaction has been extensively studied, systematic differences among the studies lead to substantial uncertainty in the recommended rate coefficient, e.g., *Sander et al.* [2011] recommend $k(233\ K) = 3.4 \times 10^{-15}$ cm^3 $molecule^{-1}$ s^{-1} (the lowest temperature of the present kinetic study) with an uncertainty factor of ~2.25 (2σ). *Green and Wayne* [1977] (187–203 nm and 298 K) and *Hubrich and Stuhl* [1980] (160–245 nm, 298 K; 160–185 nm, 208 K) have reported UV absorption spectra of HCFC-133a. There is poor agreement between these studies with differences in both the absolute cross sections and the spectrum wavelength dependence. The spectra reported by *Hubrich and Stuhl* [1980] are recommended by *Sander et al.* [2011] for use in atmospheric models.

Because of the existing discrepancies in the OH rate coefficient and UV absorption spectrum data for HCFC-133a further laboratory studies to evaluate the atmospheric impact of HCFC-133a are warranted. In this work, the rate coefficient for the OH + HCFC-133a reaction was determined over the temperature range 233−379 K using a pulsed laser photolysis-laser induced fluorescence (PLP-LIF) technique. In addition, the UV absorption spectrum of HCFC-133a was measured over the temperature range 213−323 K at 16 discrete wavelengths between 184.95 and 240 nm, the wavelength range most critical for atmospheric photolysis. The UV spectrum wavelength and temperature dependence was parameterized for use in atmospheric models. The present results are compared with results from previous studies. The Goddard Space Flight Center (GSFC) 2-D atmospheric model was used to evaluate the atmospheric loss processes, lifetimes, ODP, and the range in these values due to the uncertainties in our rate coefficient and UV spectrum laboratory data. In addition, the infrared absorption spectrum of HCFC-133a was measured and combined with the calculated lifetime to determine its GWP.

2. Experimental Details

Rate coefficients for the gas-phase OH + HCFC-133a reaction were measured as a function of temperature using pulsed laser photolysis (PLP) to produce the OH radical and laser induced fluorescence (LIF) to detect its temporal profile. Rate coefficients were measured under pseudo first-order conditions in OH, [HCFC-133a] ≫[OH], by monitoring the temporal profile of OH. The experimental apparatus and methods used in this work are described in more detail elsewhere [*Vaghjiani and Ravishankara*, 1989; *McGillen et al.*, 2013a]. The temperature of the 150 cm^3 Pyrex LIF reactor was controlled to ±0.5 K by circulating a temperature-regulated fluid through its outer jacket. Rate coefficients were measured at 233, 253, 274, 296, 324, 352, and 379 K.

OH radicals were produced by the 248 nm pulsed laser photolysis of H_2O_2 or $(CH_3)_3COOH$. The probe laser excited the $A^2\Sigma^+(v=1) \leftarrow X^2\Pi(v=0)$ OH transition at 282 nm, and its fluorescence was detected at 308 nm. Over the course of this study, the initial OH radical concentration was varied over the range $(0.3–8.5)\times10^{10}$ molecule cm^{-3} (see Table S1 in the supporting information). The OH temporal profile was measured by varying the delay between photolysis and probe lasers. Under pseudo first-order conditions, the OH temporal profile followed the relationship

$$\ln\left(\frac{[OH]_t}{[OH]_0}\right) = \ln\left(\frac{S_t}{S_0}\right) = -(k[\text{HCFC-133a}] + k_d)t = -k't \quad (1)$$

where S_t is the OH signal at time t, which is proportional to $[OH]_t$, and k' and k_d are pseudo first-order decay rate coefficients in the presence and absence of HCFC-133a, respectively. Resulting primarily from its reaction with the OH precursor and diffusion out of the detection volume, k_d represents the background loss of OH radicals in the absence of HCFC-133a. From a fit of S_t versus t, k' was obtained. At each temperature, k' was measured for a range of [HCFC-133a], and $k(T)$ was determined from the slope of k' versus [HCFC-133a], with [HCFC-133a] varied over the range $(0.31–14)\times10^{16}$ molecule cm^{-3}. Values of k_d were in the range 80–420 s^{-1}, dependent on the experimental conditions, and k_d measured in the absence of reactant agreed with the values obtained from the intercept of k' versus [HCFC-133a]. The efficient OH fluorescence quenching by HCFC-133a imposed a practical limitation on the maximum HCFC-133a concentration that could be used in our measurements.

The HCFC-133a concentration was measured online by infrared absorption using Fourier transform infrared (FTIR) absorption (1 cm^{-1} resolution) in a 15 cm long cell located at the exit of the LIF reactor. HCFC-133a concentration was determined using the integrated band strengths measured in this work, and account was taken for the pressure and temperature differences between the LIF reactor and infrared absorption cell.

The UV absorption apparatus and methods used in this work were similar to those used in recent studies from this laboratory as described elsewhere [*McGillen et al.*, 2013b]. The apparatus consisted of a 30 W deuterium lamp source, a 90.4 ± 0.3 cm long absorption cell, and a 0.25 m monochromator (150 μm entrance slit and ~1 nm (full width at half maximum) resolution) equipped with a photomultiplier tube detector. The beam path and monochromator were purged with N_2. The monochromator wavelength was calibrated using atomic lamps to an estimated accuracy of ±0.1 nm. The absorption cross section at 184.95 nm (Hg atomic line) was

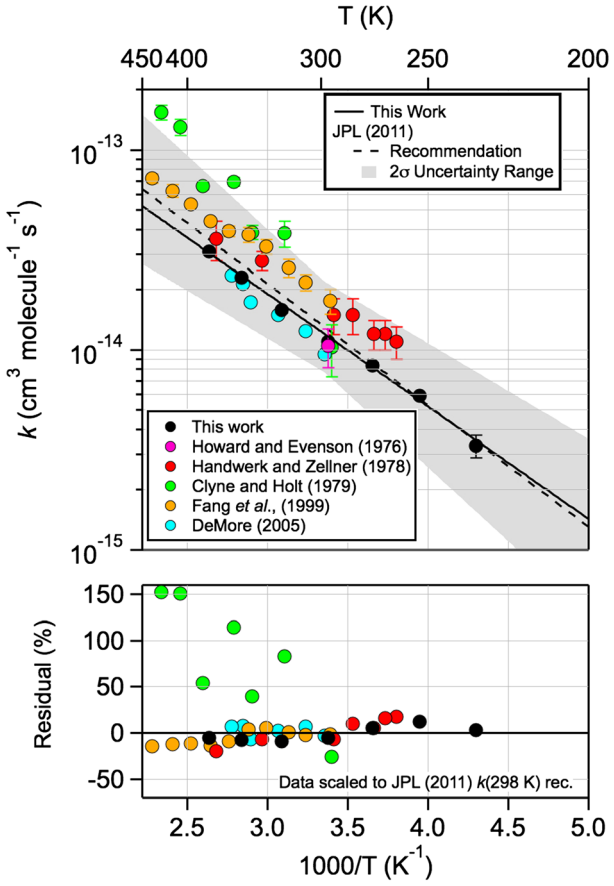

Figure 1. Rate coefficient, $k(T)$, data for the OH + CF_3CH_2Cl (HCFC-133a) reaction. (top) Present results with literature results included for comparison (see legend). (bottom) Ratio of the scaled experimental $k(T)$ data to the NASA/Jet Propulsion Laboratory (JPL) recommendation [*Sander et al.*, 2011].

measured using this setup but with a Hg Pen-Ray source and solar blind photodiode detector with 185 nm bandpass filters on the source and detector.

UV absorption cross-section measurements were made under static conditions, and [HCFC-133a] was determined using the measured total pressure of dilute gas mixtures and the ideal gas law. Absorbance (A) was measured over a range of [HCFC-133a], typically varied an order of magnitude, with concentrations in the range 2.7×10^{15} to 2.3×10^{19} molecule cm^{-3} (total pressures were in the range 10 to 760 Torr; no absorption pressure dependence was observed), dependent on the measurement wavelength. Absorption cross sections, $\sigma(\lambda,T)$, were determined using the Beer-Lambert law, $A = \sigma(\lambda,T) \times L \times$ [HCFC-133a], and a linear least squares fit of A versus [HCFC-133a]. $\sigma(\lambda,T)$ was measured at 15 discrete wavelengths between 184.95 and 240 nm at 213, 233, 253, 273, 294, and 323 K

Infrared absorption spectra were measured at 296 K between 500 and 4000 cm^{-1} at 1 cm^{-1} resolution using FTIR spectroscopy. Measurements were made using the same setup used for the [HCFC-133a] online kinetic measurements. Absorption cross sections and integrated band strengths were obtained using the Beer-Lambert law with 10 HCFC-133a concentrations in the range $(6.57–82.2) \times 10^{15}$ molecule cm^{-3}. HCFC-133a was introduced into the absorption cell from dilute gas mixtures in He (~1%, or better, mixing ratio accuracy) prepared manometrically off line. The digitized HCFC-133a infrared absorption spectrum is provided in Data Set S1 in the supporting information.

He (UHP, 99.999%), N_2 (UHP, 99.99%), and O_2 (UHP, 99.99%) were used as supplied. CF_3CH_2Cl (HCFC-133a), with a stated purity of >99.99%, was used as supplied. The H_2O_2 or $(CH_3)_3COOH$ concentration in the LIF reactor was estimated from the measured pseudo first-order decay of OH in absence of HCFC-133a. Gas flows were measured with calibrated electronic mass flow meters, and pressures were measured using 10, 100, and 1000 Torr capacitance manometers.

3. Results and Discussion

3.1. OH + HCFC-133a Rate Coefficients

A summary of the experimental conditions and rate coefficients obtained in the individual determinations is given in Table S1 in the supporting information. The rate coefficient results are also displayed in Figure 1. The 2σ precision of the $k(T)$ determination was better than 10% at all temperatures. Kinetic measurements performed at the same temperature with a variation of experimental conditions also agreed to better than 10% (see Table S1) and were combined in the final data analysis. A weighted linear least squares fit of the experimental data to an Arrhenius expression yielded $k(T) = (9.32 \pm 0.8) \times 10^{-13} \exp(-(1296 \pm 28)/T)$ cm^3 $molecule^{-1}$ s^{-1}, where the quoted uncertainties are the 2σ precision of the fit. The absolute error consists mainly of statistical

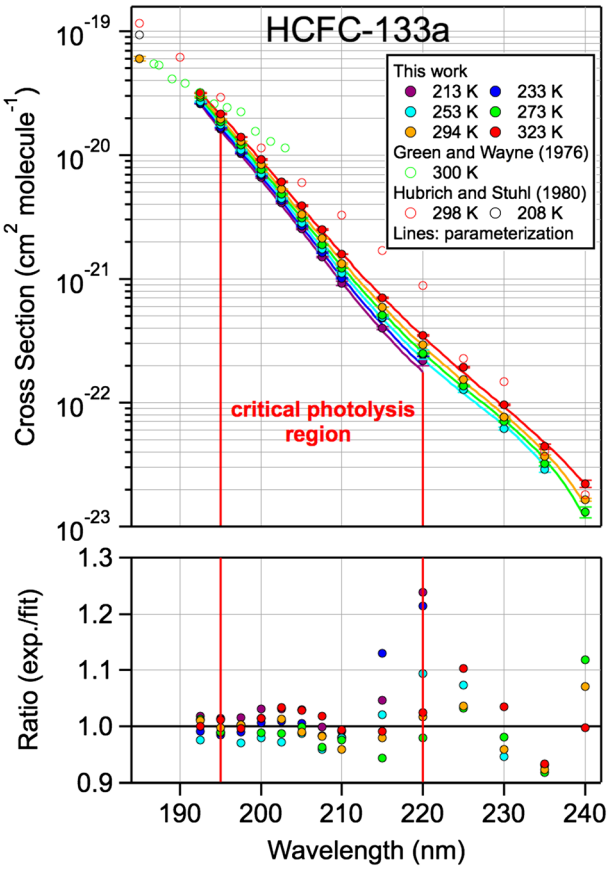

Figure 2. CF_3CH_2Cl (HCFC-133a) UV absorption spectrum. (top) Present results with literature results included for comparison (see legend). The lines were calculated from the parameterization given in Table 1. (bottom) Ratio of the present results to the parameterization given in Table 1. Results from previous studies are included for comparison (see legend).

uncertainty in the measurement of *k*, with relatively small contributions from uncertainties in [HCFC-133a], temperature, and pressure leading to an estimated overall uncertainty of 10%.

Figure 1 also includes the kinetic results from previous studies for comparison with the present results. The room temperature measurement of *Howard and Evenson* [1976] is in good agreement. Systematic differences are observed with the studies of *DeMore* [2005], *Handwerk and Zellner* [1978], *Clyne and Holt* [1979], and *Fang et al.* [1999]. For the *Handwerk and Zellner* [1978] and *Fang et al.* [1999] studies, the relative temperature dependence in *k* is comparable to the present work, although the absolute values are systematically greater by ~50% and ~75% at 298 K, respectively. There is no apparent explanation for such large differences. For the absolute study by *Clyne and Holt* [1979], although their *k*(294 K) value is in reasonable agreement with the present work, their data show large scatter and a significantly greater activation energy. The temperature dependence from the *DeMore* [2005] study is in closest agreement with the present work, although their absolute values are more scattered and differ from the present work by as much as 15%. In general there is good agreement observed between the present work and *DeMore* [2005] and *Howard and Evenson* [1976], in terms of absolute rate coefficient, and *Handwerk and Zellner* [1978] and *Fang et al.* [1999], in terms of temperature dependence. The extended temperature range of the present work has substantially reduced the uncertainty in $k(T)$ over the most important temperature range for the atmospheric loss of HCFC-133a.

3.2. HCFC-133a UV Absorption Spectrum and Parameterization

A summary of the HCFC-133a cross section data obtained in this work is given in Table S2, and the spectrum is plotted in Figure 2. The spectrum exhibits continuous absorption over the wavelength range of this study with an approximately exponential decrease in cross section with increasing wavelength. A weak inflection in the spectrum near 220 nm may indicate a contribution from a weak lower energy transition. A decrease in $\sigma(\lambda,T)$ with decreasing temperature was observed at all wavelengths in the study.

The $\sigma(\lambda,T)$ measurements obeyed the Beer-Lambert law with typical 2σ precision uncertainties of ~1%, or less, at all wavelengths studied (see Table S2). Replicate measurements that were performed using different sample mixing ratios, bath gas, range of absorption, and optical filtering agreed to within the measurement precision and were combined in the final data analysis. The overall 2σ uncertainty including estimated systematic errors was estimated to be ~4% for all wavelengths and temperatures included in this study.

Our $\sigma(\lambda,T)$ data were used to develop a spectrum parameterization based on the empirical expression given in Table 1. The fit parameters are given in Table 1, and the spectra calculated from this parameterization are included in Figure 2. The parameterization reproduces the experimental data to within ~4% over the wavelength range most critical to atmospheric photolysis, which is greater than the estimated precision of the

Table 1. CF_3CH_2Cl (HCFC-133a) UV Absorption Spectrum Parameterization From This Work Valid Over the Wavelength Range 192.5 to 240 nm for Temperatures Between 213 and 323 K[a]

$$\log_e(\sigma(\lambda,T)) = \sum_i A_i(\lambda_i - 200)^i + (T-273)\sum_i B_i(\lambda_i - 200)^i$$

i	A_i	B_i
0	−46.3107	0.003221
1	−0.18043	0.0001133
2	−0.000599	2.835×10^{-6}
3	2.4743×10^{-5}	8.007×10^{-7}
4	2.9×10^{-6}	-6.790755×10^{-8}
5	-7.149×10^{-8}	1.2007×10^{-9}

[a]The parameterization was optimized over the wavelength range 192.5 to 215 nm.

individual measurements. Extrapolation of the parameterization outside of the wavelength and temperature ranges of this study may lead to systematic errors.

The present measurements are compared with the literature values in Figure 2. The $\sigma(\lambda,296\,K)$ data of Hubrich and Stuhl are significantly greater than the present results with differences of as much as a factor of 3 at 220 nm. The spectrum reported by *Green and Wayne* [1977] also has considerable differences with our results in both the absolute cross-section values and the spectrum wavelength dependence. The reasons for these large discrepancies are unknown. *Hubrich and Stuhl* [1980] also reported cross section data at 208 K between 160 and 185 nm, which fall outside the wavelength range of the present measurements and below the wavelength range that contributes to the atmospheric photolysis of HCFC-133a.

4. Atmospheric Implications

The Goddard Space Flight Center (GSFC) 2-D atmospheric model [*Fleming et al.,* 2011] was used to quantify the atmospheric loss processes, lifetimes, ODP, and uncertainties for HCFC-133a. Calculations were performed using the OH rate coefficient Arrhenius expression and UV spectrum parameterization from this work. A unit photolysis quantum yield at all wavelengths was assumed in the calculations. The Cl and $O(^1D)$ + HCFC-133a reaction rate coefficients and other kinetic and photochemical parameters were taken from *Sander et al.* [2011]. Since the 2-D model does not include detailed tropospheric chemistry, the model tropospheric OH was specified from the monthly varying OH field documented in *Spivakovsky et al.* [2000] following the methodology outlined in *Stratospheric Processes and their Role in Climate (SPARC)* [2013]. The stratospheric and mesospheric OH, and atmospheric $O(^1D)$ and Cl atom profiles are calculated in the 2-D model. All simulations are for year 2000 steady state conditions.

Model calculations of the atmospheric loss processes of HCFC-133a, i.e., OH radical, $O(^1D)$, and Cl atom reaction and UV photolysis, are shown in Figure 3. The predominant atmospheric loss process, 98.7%, is via the H atom abstraction reaction by the OH radical. UV photolysis of HCFC-133a is a minor loss processes, ~1%, and occurs in the stratosphere almost entirely within the 190–230 nm wavelength region. The $O(^1D)$ reaction is also a minor loss process, ~0.3%, that occurs in the stratosphere. The Cl atom reaction is a negligible HCFC-133a atmospheric loss process.

The atmospheric degradation of HCFC-133a leads to the formation of CF_3CClO (via the OH reaction) and CF_3CHO (via UV photolysis and the $O(^1D)$ reaction) as predominant stable end products [*Burkholder et al.,* 2015]. *Møgelberg et al.* [1995] reported CF_3CClO to be a major (~50%) degradation product following H atom abstraction from HCFC-133a at 298 K in the presence of ~100 Torr O_2, i.e., representative of atmospheric boundary layer conditions. The CF_3CHO yield following HCFC-133a removal via UV photolysis and $O(^1D)$ reaction is expected to be near 100%. The hydrolysis of CF_3CClO and CF_3CHO leads to the formation of the persistent pollutant trifluoroacetic acid (TFA, $CF_3C(O)OH$) [*WMO,* 2014]. However, the major loss process for CF_3CHO is expected to be UV photolysis, which would not lead to TFA formation [*Chiappero et al.,* 2006].

The HCFC-133a lifetime was computed as the ratio of the annually averaged global atmospheric burden to the vertically integrated annually averaged total global loss rate [*SPARC*, 2013]. The total global lifetime was separated by the troposphere (surface to the tropopause, seasonally and latitude dependent), stratosphere, and mesosphere (<1 hPa) using the total global atmospheric burden and the loss rate integrated over the different atmospheric regions such that

$$\frac{1}{\tau_{Tot}} = \frac{1}{\tau_{Trop}} + \frac{1}{\tau_{Strat}} + \frac{1}{\tau_{Meso}} \quad (2)$$

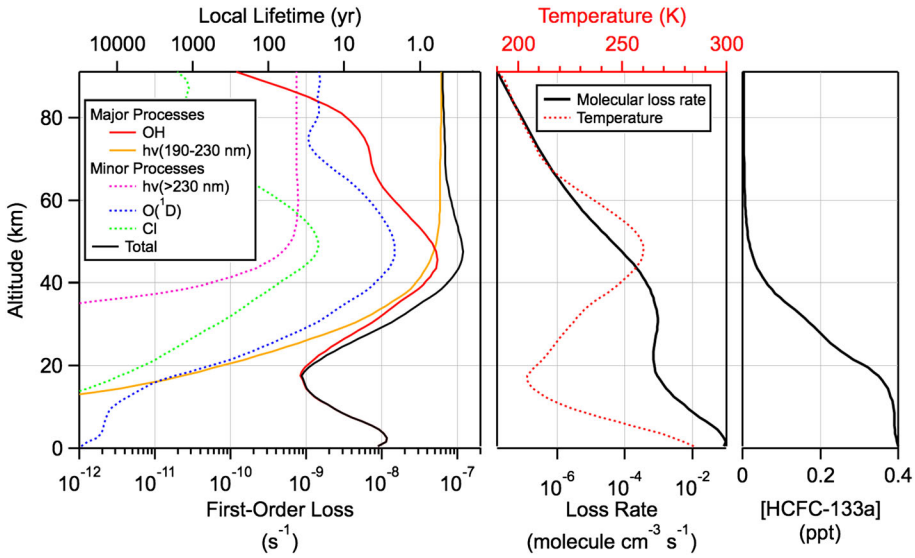

Figure 3. CF_3CH_2Cl (HCFC-133a) 2-D model results. (left) Global annually averaged loss rate coefficient (local lifetime) and contributions from individual loss processes (see legend). (middle) Molecular loss rate and temperature profile. (right) HCFC-133a mixing ratio profile.

The 2-D model total global annually averaged lifetime was calculated to be 4.45 (4.04–4.90) years. The 2σ uncertainty range in the lifetime was calculated using the absolute 2σ maximum and minimum in the OH rate coefficient and UV absorption spectrum reported in the present work, along with the 2σ uncertainties in the $O(^1D)$ and Cl atom rate coefficients taken from *Sander et al.* [2011]. The calculated lifetime is in good agreement, although slightly longer than the value estimated in *WMO* [2014] (4.0 years) that was obtained relative to the methyl chloroform lifetime. We note that the 2-D model calculated tropospheric OH lifetime for methyl chloroform (5.8 years) is similar to that given in *WMO* [2014] (6.1 years) as both methods use the tropospheric OH field from *Spivakovsky et al.* [2000]. The slightly longer 2-D model total lifetime for HCFC-133a is primarily due to the longer stratospheric lifetime as discussed below.

The tropospheric lifetime for HCFC-133a was calculated to be 4.65 (4.22–5.13) years, in agreement with the value given in *WMO* [2014] (4.5 years). The model stratospheric lifetime was 103 (95.2–110) years. This is significantly longer than the value of 35 (23–92) years reported by *Laube et al.* [2014], which was based on a tracer-tracer analysis (see *Plumb and Ko* [1992] and *Volk et al.* [1997] for method details) using a reference CFC-11 lifetime of 45 years. *WMO* [2014] reported a stratospheric lifetime of 41 years, after scaling the Laube et al. lifetime to a CFC-11 lifetime of 52 years and a very large range (27–264 years). The difference between the tracer-tracer lifetime and the present work is due, only in part, to the shorter CFC-11 lifetimes used in the tracer-tracer analyses compared to that computed in the 2-D model (57 years). Scaling the tracer-tracer result to the model CFC-11 lifetime would yield a stratospheric lifetime of ~45 years, which is still much less than the model result. The model mesospheric lifetime was quite long ($>1\times10^4$ years) due to the very small density-weighted loss rates in the mesosphere.

The model-calculated ODP for HCFC-133a was 0.017 (±0.001), where the ranges given are based on the 2σ uncertainty in the OH rate coefficient and UV spectrum from this work, along with the 2σ uncertainty in the $O(^1D)$ and Cl atom rate coefficients taken from *Sander et al.* [2011]. The ODP was calculated following the methodology used previously [*Wuebbles,* 1983*; Fisher et al.,* 1990]: separate steady state simulations (year 2000) were run with the surface boundary conditions for CFC-11 and HCFC-133a increased by 180 parts per trillion by volume (pptv) and 750 pptv, respectively, to obtain a ~1% depletion in annually averaged global total ozone. The ODP was then taken as the change in global ozone per unit mass emission of HCFC-133a relative to the change in global ozone per unit mass emission of CFC-11. The model-calculated ODP is similar to the semiempirical value of 0.02 (0.0–0.12) reported by *Laube et al.* [2014] and is close to the range listed in the Montreal Protocol (0.02–0.06). The model calculations also show that there is an extremely small uncertainty range in the ODP due solely to the uncertainty in the kinetic rate coefficients and UV spectrum obtained in this work.

4.1. HCFC-133a Infrared Absorption Spectrum and GWP Calculation

The measured infrared spectra obeyed the Beer-Lambert law with high precision, ~0.3%, and were independent of total pressure over the range 20–250 Torr (He bath gas). Strong absorption bands in the C-F stretch region were observed with an integrated band strength of $(1.16 \pm 0.003) \times 10^{-16}$ cm^2 molecule^{-1} cm^{-1} between 1070 and 1530 cm^{-1}. The present infrared spectrum agrees with that of *Etminan et al.* [2014] to within 1% from 780 to 920 cm^{-1} and to within 4% from 1070 to 1530 cm^{-1}. Integrated band strengths for these regions and the weak absorption band in the 2970–3010 cm^{-1} range are provided in the supporting information (see Table S5).

The radiative efficiency (RE) for HCFC-133a was calculated using the methods described in *Hodnebrog et al.* [2013]. The HCFC-133a radiative efficiency was calculated to be 0.16 W m^{-2} ppb^{-1}. *Hodnebrog et al.* [2013] estimate the RE calculation uncertainty to be ~25%, where the major uncertainty is due to the non-uniform vertical profile associated with compounds with less than 5 year lifetimes. On the basis of the calculated HCFC-133a lifetime from this work, the well-mixed GWPs of HCFC-133a are estimated to be 1320, 380, and 115 over the 20, 100, and 500 year time horizons, respectively, relative to CO_2 and are in good agreement with the results from *Etminan et al.* [2014] (see Table S5 for comparison).

The Gaussian 03 suite of quantum calculation programs [*Frisch et al.,* 2003] was used to estimate the infrared absorption bands at wave numbers <500 cm^{-1}, i.e., outside our measurement range, and their band strengths. Structure optimization and frequencies were calculated at MP2-6-311G(2*d*,*p*), an ab initio method with a triple-ζ quality basis set and polarization *d* and *p* functions. The calculated infrared spectra were in good agreement with our measured frequencies and band strengths. The theoretically calculated spectrum and band strengths are provided in Table S3. Low-intensity bands at 102, 180, 343, and 350 cm^{-1} were identified. The calculated bands are weak relative to the C-F stretching bands and do not contribute significantly to the radiative efficiency, ~0.2%.

5. Conclusions

Rate coefficients for the OH + CF_3CH_2Cl (HCFC-133a) reaction were measured between 233 and 379 K, which extended the low temperature range for this reaction and reduced its absolute uncertainty in the temperature range most critical to its atmospheric loss. In addition, the short-wavelength UV absorption spectrum of HCFC-133a was measured (184.95–240 nm, 213–323 K) which resolved discrepancies in previous studies. Two-dimensional model calculations were used to assess the atmospheric loss processes of HCFC-133a as well as its atmospheric lifetime and ozone depletion potential (ODP).

OH reactive loss was shown to be the predominant loss process, and a total global annually averaged lifetime of 4.45 years was obtained with a 2σ uncertainty range of 4.04–4.90 years. The lifetime obtained in the 2-D model calculations agrees with the recommended value in *WMO* [2014] that was obtained using the methyl chloroform reference method. The model-calculated lifetime uncertainty range is based on the 2σ uncertainty range in the OH rate coefficient and UV absorption spectrum reported in this work; the contributions from the O(^{1}D) and Cl rate coefficient uncertainties are extremely small. The model tropospheric lifetime for HCFC-133a was calculated to be 4.65 (4.22–5.13) years. The model stratospheric lifetime 103 (95.2–110) years is significantly longer than the *Laube et al.* [2014] estimated value of 35 (23–92) years, which was based on a tracer-tracer analysis.

The 2-D model calculated ODP was 0.017 with a 2σ uncertainty of ±0.001. The model calculations show an extremely small uncertainty range in the ODP due to the uncertainty in the kinetic rate coefficients and UV spectrum reported in this work. This value is close to the range listed in the Montreal Protocol (0.02–0.06) and is typical of HCFCs with atmospheric lifetimes less than 5 years [*WMO,* 2014]. On the basis of our measured HCFC-133a infrared spectrum and 2-D model calculated lifetimes, well-mixed GWPs for HCFC-133a were calculated to be 1300, 374, and 114 over the 20, 100, and 500 year time horizons, respectively, relative to CO_2. These values are consistent with the values given in *WMO* [2014].

Acknowledgments
This work was supported in part by NOAA's Atmospheric Chemistry, Carbon Cycle, and Climate (AC4) Program and NASA's Atmospheric Composition Program. Supporting data are included as a data set and as one figure and five tables in an SI file; any additional data may be obtained from J.B.B. (email: James.B.Burkholder@noaa.gov).

The Editor thanks Timothy J. Wallington and an anonymous reviewer for their assistance in evaluating this paper.

References

Burkholder, J. B., R. A. Cox, and A. R. Ravishakara (2015), Atmospheric degradation of ozone depleting substances, their substitutes, and related species, *Chem. Rev.*, doi:10.1021/cr5006759.

Chiappero, M. S., F. E. Malanca, G. A. Arguello, S. T. Wooldridge, M. D. Hurley, J. C. Ball, T. J. Wallington, R. L. Waterland, and R. C. Buck (2006), Atmospheric chemistry of perfluoroaldehydes ($C_xF_{2x+1}CHO$) and fluorotelomer aldehydes ($C_xF_{2x+1}CH_2CHO$): Quantification of the important role of photolysis, *J. Phys. Chem. A*, *110*, 11,944–11,953.

Clyne, M. A. A., and P. M. Holt (1979), Reaction-kinetics involving ground $X^2\Pi$ and excited $A^2\Sigma^+$ hydroxyl radicals: 2. Rate constants for reactions of OH $X^2\Pi$ with halogenomethanes and halogenoethanes, *J. Chem. Soc. Faraday Trans. 2*, *75*, 582–591.

DeMore, W. B. (2005), Regularities in Arrhenius parameters for rate constants of abstraction reactions of hydroxyl radical with C–H bonds, *J. Photochem. Photobiol. A*, *176*, 129–135.

Etminan, M., E. J. Highwood, J. C. Laube, R. McPheat, G. Marston, K. P. Shine, and K. M. Smith (2014), Infrared absorption spectra, radiative efficiencies, and global warming potentials of newly-detected halogenated compounds: CFC-113a, CFC-112 and HCFC-133a, *Atmosphere*, *5*, 473–483.

Fang, T. D., P. H. Taylor, and R. J. Berry (1999), Kinetics of the reaction of OH radicals with CH_2ClCF_2Cl and CH_2ClCF_3 over an extended temperature range, *J. Phys. Chem. A*, *103*, 2700–2704.

Fisher, D. A., C. H. Hales, D. L. Filkin, M. K. W. Ko, N. D. Sze, P. S. Connell, D. J. Wuebbles, I. S. A. Isaksen, and F. Stordal (1990), Model calculations of the relative effects of CFCs and their replacements on stratospheric ozone, *Nature*, *344*(6266), 508–512.

Fleming, E. L., C. H. Jackman, R. S. Stolarski, and A. R. Douglass (2011), A model study of the impact of source gas changes on the stratosphere for 1850–2100, *Atmos. Chem. Phys.*, *11*, 8515–8541.

Frisch, M. J., et al. (2003), *Gaussian 03, Revision B.02*, Gaussian, Pittsburgh, Pa.

Green, R. G., and R. P. Wayne (1977), Vacuum ultra-violet spectra of halogenated methanes and ethanes, *J. Photochem.*, *6*, 375–377.

Handwerk, V., and R. Zellner (1978), Kinetics of reactions of OH radicals with some halocarbons ($CHClF_2$, CH_2ClF, CH_2ClCF_3, CH_3CClF_2, CH_3CHF_2) in temperature range 260 K–370 K, *Ber. Bunsen-Ges. Phys. Chem.*, *82*, 1161–1166.

Hodnebrog, Ø., M. Etminan, J. S. Fuglestvedt, G. Marston, G. Myhre, C. J. Nielsen, K. P. Shine, and T. J. Wallington (2013), Global warming potentials and radiative efficiencies of halocarbons and related compounds: A comprehensive review, *Rev. Geophys.*, *51*, 300–378, doi:10.1002/rog.20013.

Howard, C. J., and K. M. Evenson (1976), Rate constants for reactions of OH with ethane and some halogen substituted ethanes at 296 K, *J. Chem. Phys.*, *64*, 4303–4306.

Hubrich, C., and F. Stuhl (1980), The ultraviolet absorption of some halogenated methanes and ethanes of atmospheric interest, *J. Photochem.*, *12*, 93–107.

Laube, J. C., et al. (2014), Newly detected ozone-depleting substances in the atmosphere, *Nat. Geosci.*, *7*, 266–269.

Manzer, L. E. (1990), The CFC-ozone issue: Progress on the development of alternatives to CFCs, *Science*, *249*, 31–35.

McGillen, M. R., M. Baasandorj, and J. B. Burkholder (2013a), Gas-phase rate coefficients for the OH + n-, i-, s-, and t-butanol reactions measured between 220 and 380 K: Non-arrhenius behavior and site-specific reactivity, *J. Phys. Chem. A*, *117*, 4636–4656.

McGillen, M. R., E. L. Fleming, C. H. Jackman, and J. B. Burkholder (2013b), $CFCl_3$ (CFC-11): UV absorption spectrum temperature dependence measurements and the impact on its atmospheric lifetime and uncertainty, *Geophys. Res. Lett.*, *40*, 4772–4776, doi:10.1002/grl.50915.

Miller, M., and T. Batchelor (2012), Information paper on feedstock uses of ozone-depleting substances, 72 pp. [Available at http://ec.europa.eu/clima/policies/ozone/research/docs/feedstock_en.pdf.]

Møgelberg, T. E., O. J. Nielsen, J. Sehested, and T. J. Wallington (1995), Atmospheric chemistry of HCFC-133a: The UV absorption spectra of CF_3CClH and CF_3CClHO_2 radicals, reactions of CF_3CClHO_2 with NO and NO_2, and fate of CF_3CClHO radicals, *J. Phys. Chem.*, *99*, 13,437–13,444.

Plumb, R. A., and M. K. W. Ko (1992), Interrelationships between mixing ratios of long-lived stratospheric constituents, *J. Geophys. Res.*, *97*, 10,140–10,156.

Sander, S. P., et al. (2011), Chemical kinetics and photochemical data for use in atmospheric studies, JPL Publication 10-6, Evaluation Number 17.

Stratospheric Processes and their Role in Climate (SPARC) (2013), SPARC Report on the Lifetimes of Stratospheric Ozone-Depleting Substances, 993 Their Replacements, and Related Species, *SPARC Rep. 6, WCRP-15/2013*, edited by M. Ko et al. [Available at http://www.sparc-climate.org/publications/sparc-reports/sparc-report-no6/.]

Spivakovsky, C. M., et al. (2000), Three-dimensional climatological distribution of tropospheric 997 OH: Update and evaluation, *J. Geophys. Res.*, *105*, 8931–8980, doi:10.1029/1999JD901006.

United Nations Environment Programme (2012), *May 2012 Report of the Technology and Economic Assessment Panel*, *Prog. Rep.*, 222 pp., vol. 1, Nairobi, Kenya. [Available at http://montreal-protocol.org/Assessment_Panels/TEAP/Reports/TEAP_Reports/teap-progress-report-may2012.pdf.]

Vaghjiani, G. L., and A. R. Ravishankara (1989), Kinetics and mechanism of OH reaction with CH_3OOH, *J. Phys. Chem.*, *93*, 1948–1959.

Volk, C. M., J. W. Elkins, D. W. Fahey, D. S. Dutton, J. M. Gilligan, M. Loewenstein, J. R. Podolske, K. R. Chan, and M. R. Gunson (1997), Evaluation of source gas lifetimes from stratospheric observations, *J. Geophys. Res.*, *102*, 25,543–25,564, doi:10.1029/97JD02215.

World Meteorological Organization (2014), *Scientific Assessment of Ozone Depletion: 2014*, *Global Ozone Res. Monit. Proj.-Rep. 55*, 416 pp., Geneva, Switzerland. [Available at http://www.wmo.int/pages/prog/arep/gaw/ozone_2014/ozone_asst_report.html.]

Wuebbles, D. J. (1983), Chlorocarbon emission scenarios: Potential impact on stratospheric ozone, *Geophys. Res. Lett.*, *88*, 1433–1443, doi:10.1029/JC088iC02p01433.